ELSEVIER

Automation in Construction 15 (2006) 47 – 57

AUTOMATION IN CONSTRUCTION

www.elsevier.com/locate/autcon

Segmentation of buried concrete pipe images

Sunil K. Sinha [a,*], Paul W. Fieguth [b]

[a] Department of Civil and Environmental Engineering, Pennsylvania State University, University Park, PA 16802, USA
[b] Department of Systems Design Engineering, University of Waterloo, ON, Canada N2L3G1

Accepted 4 February 2005

Abstract

The enormity of the problem of deteriorating pipeline infrastructure is widely apparent. Since a complete rebuilding of the piping system is not financially realistic, municipal and utility operators require the ability to monitor the condition of buried pipes. Thus, reliable pipeline assessment and management tools are necessary to develop long term cost effective maintenance, repair, and rehabilitation programs. In this paper a simple, robust and efficient image segmentation algorithm for the automated analysis of scanned underground pipe images is presented. The algorithm consists of image pre-processing followed by a sequence of morphological operations to accurately segment pipe cracks, holes, joints, laterals, and collapsed surfaces, a crucial step in the classification of defects in underground pipes. The proposed approach can be completely automated and has been tested on five hundred scanned images of buried concrete sewer pipes from major cities in North America.

Keywords: Pipeline infrastructure; Automated inspection; Pipeline assessment; Image processing; Segmentation; Mathematical morphology

1. Introduction

Most municipal pipeline systems are inspected visually by mobile Closed Circuit Television (CCTV) systems or by human inspectors [1]. There are several CCTV variants that may reduce the cost of the inspection or provide improved results each using a television camera in conjunction with a video monitor, videocassette recorders, and possibly other recording devices, and falling into one of two basic types [2]: either the inspection is performed using a stationary or zoom camera mounted at a manhole so that it looks down the pipe, or a mobile robotic system is placed within the pipe itself. A typical pan and tilt CCTV camera and the corresponding image from an internal inspection of a buried sewer pipe are shown in Fig. 1. The camera provides images to an operator who is trained to detect, classify and rate the severity of defects against documented criteria [3]. Manual CCTV inspection has been shown to be incapable of performing reliable inspection [4], since the human vision process is prone to subjective considerations, fatigue, boredom, lapses in operator concentration and inexperience [2]. Thus, manual results are widely agreed to lack reliability and consistency, precluding the undertaking of preventive maintenance with confidence.

The sewer scanner and evaluation technology (SSET) [3] is an innovative technology for obtaining images of the interior of pipe, developed by TOA Grout, CORE Corp., Japan, and the Tokyo Metropolitan Sewer Authority. SSET is a system that offers a new inspection method, utilizing digital optical scanning and gyroscopic technology, minimizing some of the shortcomings of traditional CCTV inspection equipment. The mechanics of inspecting the pipes by SSET are similar to the CCTV inspection, in that the SSET probe is designed to operate from a tractor platform to propel the tool through the pipe. The SSET probe and digitized images of underground pipe with various objects are shown in Fig. 2. The major benefit of the SSET system over the current CCTV technology is that the engineer will have much higher quality image data to make critical rehabilitation decisions, and the flattened

* Corresponding author. Tel.: +1 814 865 9433; fax: +1 814 863 7304.
E-mail addresses: sunil@engr.psu.edu (S.K. Sinha), pfieguth@uwaterloo.ca (P.W. Fieguth).

0926-5805/$ - see front matter © 2005 Elsevier B.V. All rights reserved.
doi:10.1016/j.autcon.2005.02.007

Fig. 1. CCTV camera and internal inspection image of buried pipelines.

image geometry, greatly simplifying automated computer-based analyses.

The goal of our research is to develop an automated method which, given a pipe image, classifies each object in the image into one of five classes: background, crack, hole, joint, and lateral.

2. Buried pipe image pre-processing

We have acquired a data set consisting of thousands of images of buried sewer concrete pipes from major cities in North America. This data set has been used to explore basic characteristics of underground pipe images. Analyses of images have shown that there are two important characteristics that complicate the segmentation of pipe images: firstly the presence of a complicated background pattern due to earlier runoff, patches of repair work, corroded areas, debris, non-uniformities in illumination, and flaws in the image acquisition process; secondly the three main objects of interest–cracks, joints, and laterals–are all dark features that cannot be distinguished by intensity criteria alone (Fig. 3).

There are several challenges in analyzing and classifying these pipe images. First is the difficulty in developing a mathematical model for each object of interest, straightforward for regular, known structures such as joints and laterals, but much harder for random, irregular holes and joints. Next is the challenge of the background, often highly patterned and cluttered, leading to spuriously detected edges. Finally is the problem of limited contrast, particularly between minor cracks and the background. Thus the use of digital image data typically requires some degree of preprocessing, including geometric correction, image enhancement, and feature selection [5–7]. For example, geometric correction involves the reorientation of the image data to selected parameters [8], allowing for accurate spatial assessments and measurements of crack features. Image enhancement seeks an improvement of the image data that suppresses unwanted distortions in background or enhances some image features (like cracks) important for further processing. The principal objective of image pre-processing is to process an image so that the result is more suitable than the original image for a specific application. The word 'specific' is important, because it establishes at the outset that the techniques discussed in this section are very much problem-oriented. In this section, we examine image pre-processing for contrast enhancement.

2.1. Bayesian classification

The identification of the boundary between objects and their surroundings can be formulated as a pattern classi-

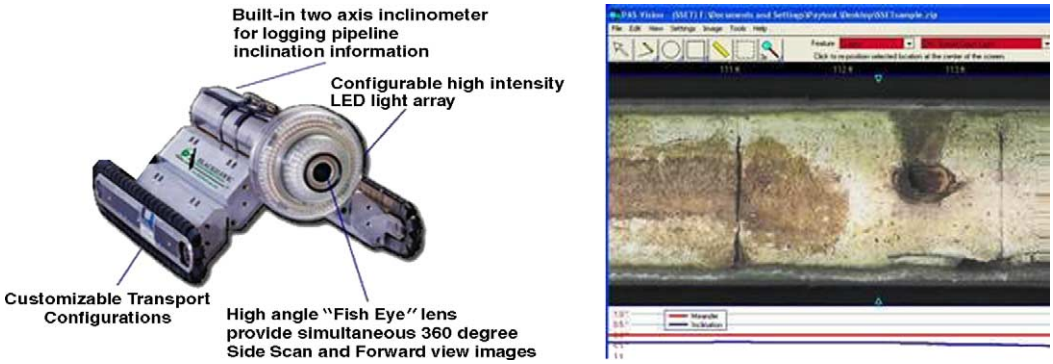

Fig. 2. SSET inspection probe and digitized color image of buried pipe surface.

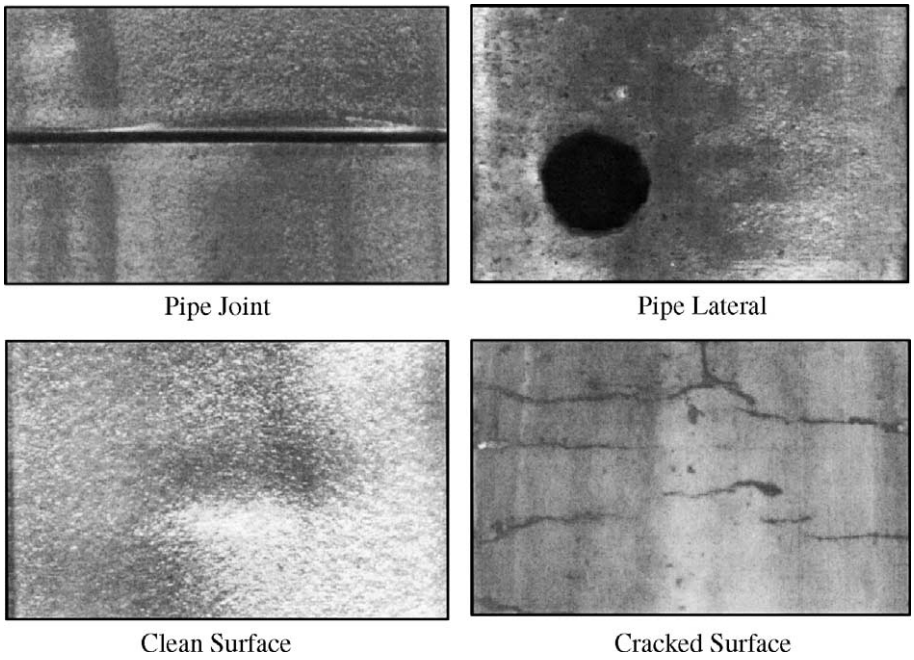

Fig. 3. Typical SSET images of underground concrete pipe showing different objects.

fication problem [9]. Specifically, it is desired to classify a pixel as to whether it is more likely that it came from same object or the neighboring background. In a Bayesian framework, a color pixel $x_c=(r,g,b)^T$, can be classified as a crack if its a posteriori probability $P(\text{Crack}|x)$ is greater than the corresponding a posteriori probability for the surrounding pipe background $P(\text{Back}|x)$. If the class-conditional probability densities $p(x|\text{Crack})$ and $p(x|\text{Back})$ are known, then Bayes' Rule can be used to compute the corresponding a posteriori probabilities.

Standard parametric or non-parametric techniques can be used to learn the underlying class-conditional densities $p(x|\text{Crack})$ and $p(x|\text{Back})$. However, one must bear in mind that the a posteriori probabilities $P(\text{Crack}|x)$ and $P(\text{Back}|x)$ are evaluated for each pixel, along each search line, at each time step. Thus, in order for this approach to be usable in practical (real-time) systems, a premium is placed on the on-line processing time required to discriminate between the classes. Towards this end, Fisher's linear discriminant [10] is used to enhance the contrast between the objects and the pipe background. In the case of a two class discrimination problem, such as distinguishing between objects and pipe background, Fisher's linear discriminant [10] can be used to determine the axis, w, onto which vector color data can be projected which preserves as much of the discriminating capability of the color information as possible. The resulting 'Fisher linear discriminant' maximizes the separability of the two classes. Crack images representative of those likely to be encountered during scanning of underground pipes can be used to learn the Fisher discriminant axis.

$$w = (S_c + S_B)^{-1}(m_C - m_B) \tag{1}$$

where S and m are the class scatter and mean, respectively.

$$m_k = \frac{1}{n_k}\sum_{x\in\chi_k} x \tag{2}$$

$$S_k = \sum_{x\in\chi_k}(x-m_k)(x-m_k)^T \tag{3}$$

Computed over all samples x_k in class k.

Fig. 4 shows how Fisher's discriminant analysis can be used to enhance the contrast between the pipe background and cracks, comparing the original color image, its gray-scale equivalent, and the enhanced projection onto the Fisher axis.

3. Segmentation of buried pipe images

In our proposed automated pipe analysis the following need to be discriminated: pipe joints (a horizontal dark straight line), pipe lateral (a circular dark object), surface cracks (randomly shaped thin dark lines), and pipe background (highly patterned). Successfully segmenting pipe joints, laterals, and cracks, all of which are dark, will clearly require some discrimination on the basis of geometry and shape. In this paper a morphological segmentation approach, based on set-theoretic concepts of shape [11], is proposed for extracting joints and laterals. The main objective of this approach is to segment out the pipe joints and laterals from the image, at which point the subtle surface cracks can be more readily extracted by a subsequent filtering operation [12,34].

A large number of segmentation algorithms have been proposed in the literature [13–16], however the literature on

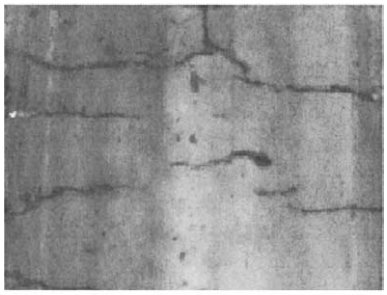

(a) Original Color Image

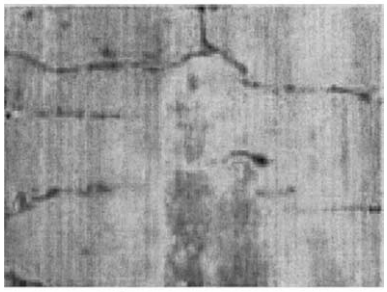

(b) Gray-scale Image

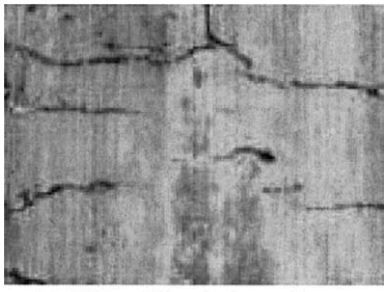

(c) Fisher Discriminant Image

Fig. 4. Fisher's discriminant analysis can be used to enhance the contrast between the pipe background and cracks. The original color image (a) shows few cracks in the pipe surface. In gray-scale image (b) there is little contrast between the background and crack. Projection onto a Fisher axis (c) enhances the contrast and enables better extraction of the crack features.

segmentation of concrete pipe defects is very limited. Maser's algorithm [17] recommends a histogram thresholding approach, however it is not clear how the value of the threshold is originally determined. More recently, Chen et al. [18] applied a segmentation method, introduced by Kittler et al. [19], to pavement images, although the effectiveness of the method is unclear. An approach to the recognition of segmented pavement distress images is studied by Mohajeri and Manning [20], using directional filters to classify the objects. An entropy-based approach [11], which finds a bilevel threshold to maximize entropy criteria, did not improve pavement-surface images. The cluster classification process, which assigns a particular object to one of many groups by comparing typical features from each group, reported a significant amount of error [12].

In general, segmentation techniques take one of three possible approaches [21]: edge detection, thresholding, or object geometry. An edge is defined as the boundary between two regions with relatively distinct gray-scale characteristics, thus edge-detection techniques attempt to segment objects by outlining their boundaries. Thresholding, on the other hand, seeks to distinguish objects on the basis of their absolute intensities, for example separating a darker object from a lighter background. The literature on segmentation based on gray-level intensity is inapplicable in our context since cracks, holes, joints, and laterals all appear as comparably dark objects on a lighter background, as shown in Fig. 3. Rather, it is the *geometry*, rather than the intensity, which distinguishes these objects. Mathematical morphology [22–26] provides an approach to the segmenting of digital images that is based on *shape*. Appropriately used, morphological operations tend to simplify images, preserving their essential shape characteristics and eliminating irrelevancies.

4. Mathematical morphology

Mathematical morphology [22–27] is a widely used methodology for image analysis, smoothing, segmentation, edge detection, thinning, shape analysis and coding. Based on a formal mathematical framework, mathematical morphology is a fast, robust method that analyzes the geometry of an image directly in the spatial domain. In this section, we present a morphological approach for segmenting underground pipe images, which includes the process of characterizing the object sizes in a pipe image, thresholding the image into a binary image, and finally classifying the segmented image. Morphology operates on image regions (e.g., the light and dark portions of an image), where the regions can be reshaped (i.e., morphed) in various ways under the control of a structuring element. The structuring element can be thought of as a parameter to the morphological operation. The most fundamental operations are morphological *dilation* and *erosion*. Based on these, two compound operations, *opening* and *closing*, can be defined. We first define these in the context of binary images, then for gray-scale images.

Consider a binary image $I=\{p(x,y)\}$ consisting of pixels $p(x,y)\in\{0,1\}$.

We define sets A and B to represent the image and the selected structuring element, respectively:

$$A=\{(x,y)|p(x,y)=1\} \tag{4}$$

$$B=\{(x,y)|(x,y) \text{ in structuring element}\} \tag{5}$$

Then the *dilation* $A\oplus B$ of A by B is defined as

$$AB=\{a+b| \text{ for all } a\in A \text{ and } b\in B\} \tag{6}$$

That is, $A\oplus B$ is the union of all pixels in A surrounded by the shape of B. Similarly the *erosion* $A\Theta B$ is defined as

$$A\Theta B=\{p|b+p\in A \text{ for every } b\in B\} \tag{7}$$

That is, all pixels within a "distance" B from the edge of A are removed. Next, two compound operations can be defined, *opening* $A \circ B$ and closing $A \bullet B$:

$$A \circ B = (A \ominus B) \oplus B \tag{8}$$

$$A \bullet B = (A \oplus B) \ominus B \tag{9}$$

The opening operation, which we use in our classification, leaves unchanged all parts of A, except for those features and regions smaller than the structuring element, which are removed. Any method which operates exclusively on binary images is somewhat limiting, since most images are color or gray-scale. A gray-scale image $I = \{p(x,y)\}$, $p(x,y) \in \Re$ can be interpreted as a three-dimensional surface, with the pixel intensity or shade interpreted as a height. If we define

$$A = \{(x,y,z) | z \leq p(x,y)\} \tag{10}$$

and given some structuring volume B, then we can interpret two-dimensional gray-scale morphological operations on image I as three-dimensional binary morphology on A, B. Written directly in terms of a gray-scale image $f(x,y)$ and structuring function $b(x,y)$, grey-scale *erosion* and *dilation* [35] can be defined as

$$(f \oplus b)(x,y) = \max_{(i,j)} \{f(x-i, y-j) + b(i,j)\} \tag{11}$$

$$(f \ominus b)(x,y) = \max_{(i,j)} \{f(x+i, y+j) - b(i,j)\} \tag{12}$$

The gray-scale opening and closing are then defined as before, in Eqs. (8) and (9).

5. Morphological segmentation

In underground pipe image segmentation, the following classes are of general interest: the pipe joints (horizontal dark straight lines), pipe laterals (circular dark objects), surface cracks (irregularly shaped thin dark lines), and the pipe background (anywhere from a smooth to a highly patterned surface). The goal of our research is to segment pipe joints, laterals, and cracks based on the *geometric* differences between them, specifically based on morphology.

The premise of the morphological approach is to distinguish objects on the basis of shape. With the canonical shapes being thin and wide (joints), large and round (laterals), and small and irregular (cracks, holes), the key idea of this paper is to use two parameterized structuring

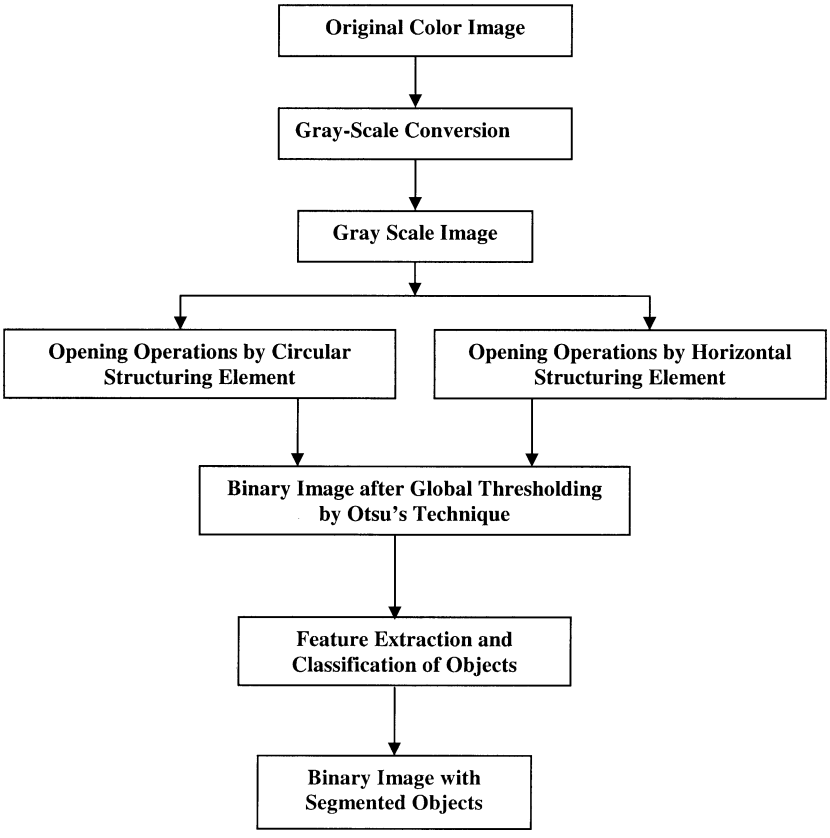

Fig. 5. Overview of the proposed morphological segmentation approach.

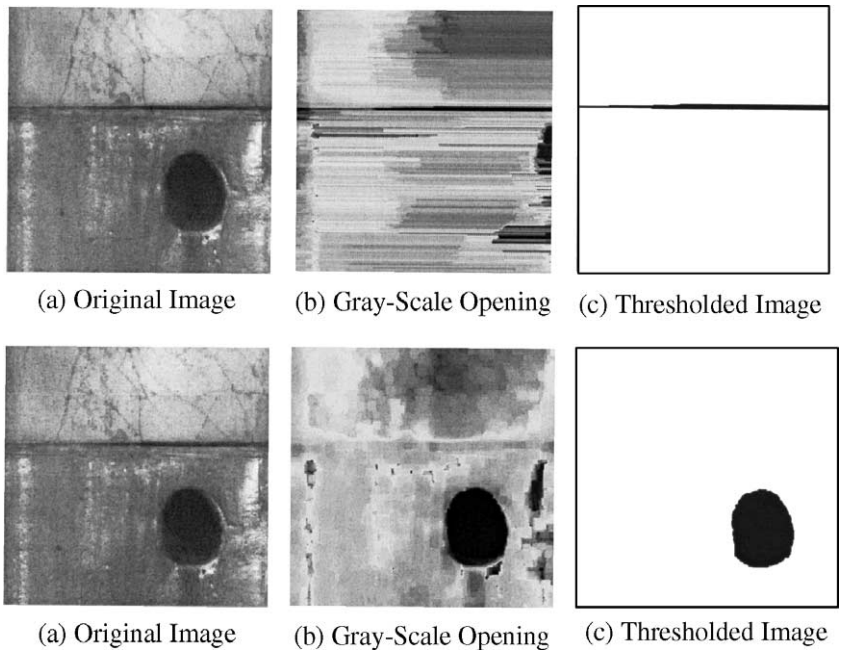

Fig. 6. This figure illustrates joint/lateral discrimination using different structuring element: a horizontal element (top) of length 285 mm, consistent with the geometry of a perfect joint, as opposed to a circular element (bottom) of radius 57 mm, tuned to the shape of a perfect lateral.

elements: a circular structuring element (S_C) of radius r, and a horizontal structuring element (S_H) of varying length l and fixed width $w=3$. As the effect of an opening is to remove those features, which are small relative to the structuring element S while preserving features greater than S, the choice of these two elements (circular and rectangular) is clearly designed to mimic the geometry of the laterals and joints to be extracted. The key idea, then, is that we can isolate objects of a given 'size' by performing a series of opening operations, based on structuring elements of varying size. The 'size' of any object can then be defined mathematically as the largest structuring element (measured here in terms of radius r or length l) that can be inscribed in the object. Note that, aside from the general shape of the structuring element, we do not make any specific assumption regarding the shape of the object being measured, therefore this definition of size is quite general and will prove effective in measuring sizes of cracks, irregular laterals, etc., which otherwise resist specific characterization. The segmentation algorithm consists of a sequence of processing steps, illustrated in Fig. 5, and developed below.

5.1. Morphological opening and thresholding

We performed a morphological opening operation on the underground pipe image with increasing sizes of the circular and horizontal structuring elements. Clearly as the size of the structuring element is increased features of increasing size are removed by the morphological opening. For example, a structuring element of intermediate size will preserve laterals and a collapsed pipe, but will remove cracks and small holes.

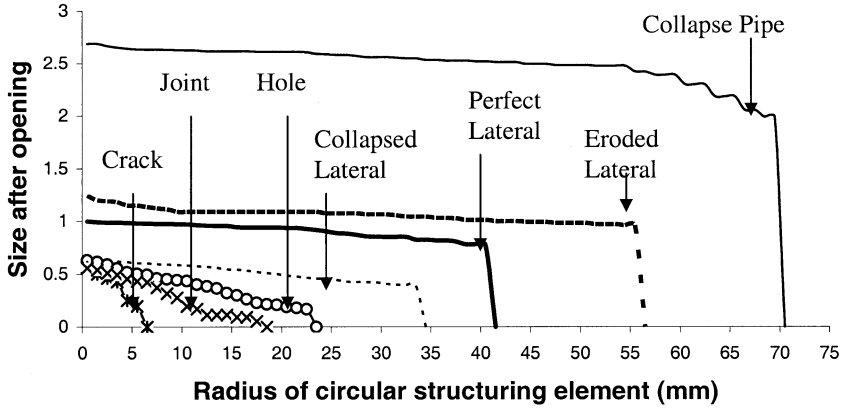

Fig. 7. Morphological analysis based on a circular structuring element: the average area of each class is plotted as a function of the structuring element diameter; area is normalized to that of an ideal lateral. Clearly as the diameter is increased, classes with thin, elongated geometries (e.g. cracks, joints) are quickly eliminated.

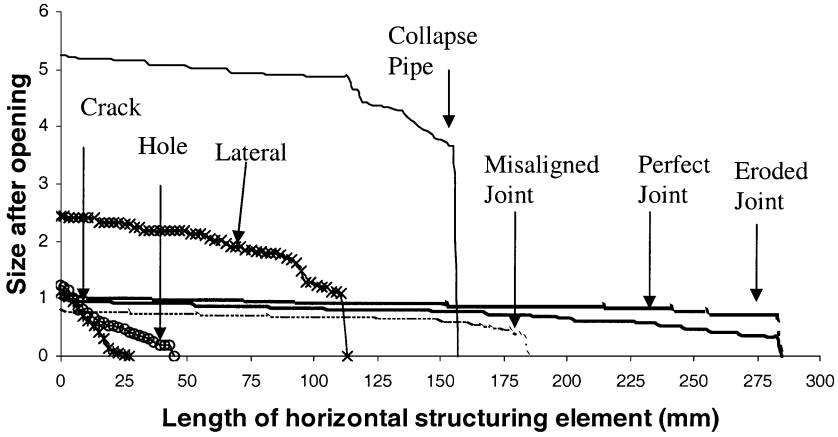

Fig. 8. As in Fig. 7, but using a horizontal structuring element, normalized to the area of an ideal joint. Clearly as the length is increased, classes with small geometries (e.g., cracks, holes) are quickly eliminated.

Fig. 6(b) shows two examples of the results of gray-scale opening. Although some of the original features in Fig. 6(a) are still clearly present, the output of the morphology is confusing and not easily interpreted. What we really want is an additional processing step, a thresholding function $t()$, classifying each pixel as:

$$t(p(x,y)) = \left\{ \begin{array}{ll} 0 & \text{Pixel is geometrically consistent with structuring element} \\ 1 & \text{Pixel is not consistent} \end{array} \right\} \tag{13}$$

That is, the set of all 'dark' (zero valued) pixels will identify the object(s) in the image which are compatible (i.e., bigger than) the selected structuring element. Ideally, we would like a single global threshold T such that

$$t(p(x,y)) = \left\{ \begin{array}{ll} 0 & p(x,y) \le T \\ 1 & p(x,y) \ge T \end{array} \right\} \tag{14}$$

Unfortunately, it is difficult in general to find a single threshold that is best for an arbitrary gray-scale image. Many approaches have been proposed to find an optimal threshold level for certain image cases [28–31]. We propose to use Otsu's method [30] because it is non-parametric, unsupervised, and automatic. A discriminant criterion is computed for each possible threshold T; the optimal threshold is that gray-level where this measure is maximized. The results of Otsu's method are illustrated in Fig. 6(c): the segmented joint and lateral stand out very clearly. With a methodology in place for understanding the results of a given morphology, we can now study the choice of structuring elements that will be most effective in classifying each pipe object. Figs. 7 and 8 plot the average area of objects in each class (crack, hole, joint, etc.) based on circular and horizontal structuring elements, respectively. That is, if we let $|t(I)|$ represent the number of dark pixels in I after binary thresholding, then Figs. 7 and 8 actually plot the normalized areas

$$a_{\mathrm{L}}(r) = \frac{|t(I \circ S_{\mathrm{C}}(r))|}{|t(I_{\mathrm{L}})|} \qquad a_J(l) = \frac{|t(I \circ S_{\mathrm{H}}(l))|}{|t(I_{\mathrm{J}})|} \tag{15}$$

where I_{L}, I_{J} are idealized, prototype images of the perfect lateral and joint. Note that all of the curves are monotonically decreasing,

$$|I \circ S_{\mathrm{C}}(r_1)| \ge |I \circ S_{\mathrm{C}}(r_2)| \text{ for all } r_1 \le r_2 \tag{16}$$

since a larger structuring element cannot leave more pixels in place than a smaller element.

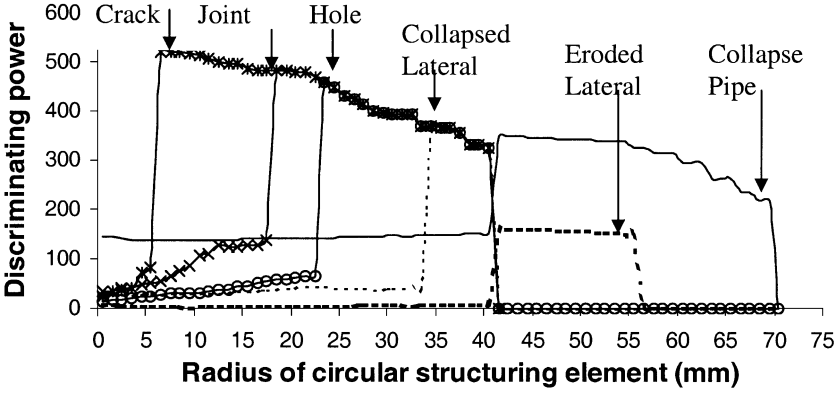

Fig. 9. Lateral discrimination: we can distinguish between laterals and other classes by opening with a circular structuring element. We can plot the ability to discriminate D between an ideal lateral and any other class as the difference in response (normalized to standard error) to the structuring element.

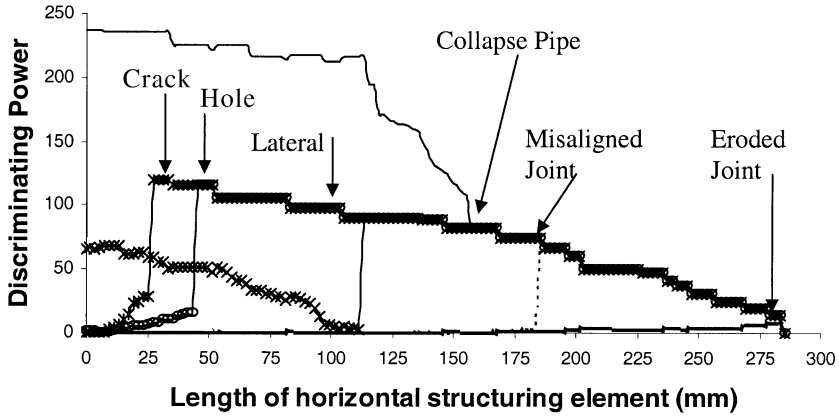

Fig. 10. Joint discrimination: as in Fig. 9, but using a horizontal structuring element. We can plot the ability to discriminate D between an ideal joint and any other class as the difference in response (normalized to standard error) to the structuring element.

Although the plots in Figs. 7 and 8 are interesting and intuitive, in order to accurately isolate and classify different objects in an image we have to take into account the *variations* in the area of each class. That is, holes, laterals, etc. all come in a range of sizes, and this range *must* be taken into account in selecting the appropriate structuring element to serve as a classifier.

We can compute or assess the ability of any structuring element to discriminate between any two classes (e.g., crack and hole) by examining the $D_{i,j}$ degree to which two classes are separated relative to their standard deviations:

$$D_{i,j}(r) = \frac{|\mu_i(r) - \mu_j(r)|^2}{\sigma_i^2(r) + \sigma_j^2(r)} \tag{17}$$

$$\mu_i(r) = \langle a_{\mathrm{L}}(r)\rangle_i \text{ and } \sigma_i^2(r) = \langle a_{\mathrm{L}}|(r)^2\rangle_i - \langle a_{\mathrm{L}}(r)\rangle_i^2 \tag{18}$$

where $\langle\rangle_i$ represents an average taken over images of class i. A parallel definition exists for discriminant $D_{i,j}(l)$ based on a horizontal structuring element. The value of r for which $D_{i,j}(r)$ is maximized represents the optimal feature by which to discriminate between classes i and j on the basis of the area (i.e. number of pixels) remaining after a morphological opening by element $S_{\mathrm{C}}(r)$. By plotting $D_{i,j}(r)$ and $D_{i,j}(l)$ for different classes i,j we can deduce the set of features to be extracted for classification. Figs. 9 and 10 plot $D_{\mathrm{L},i}(r)$ and $D_{\mathrm{J},i}(l)$, respectively, indicating peaks to identify these features.

5.2. Feature extraction and classification

The sizes of structuring elements for the classification of objects in underground pipe images can be determined from the discriminant method described in the previous section. For example, if an image is opened with $S_{\mathrm{C}}(2)$–the circular structuring element of radius 2(mm)–then small objects (e.g., random background patterning) are removed. By repeating this process for different sizes of structuring elements $S_{\mathrm{C}}(7)$, $S_{\mathrm{C}}(23)$, $S_{\mathrm{C}}(57)$, we can group objects by size, that is, into their respective classes.

Specifically, we propose to keep as our features

$$a_{\mathrm{L}}(r) = |t(I \circ S_{\mathrm{C}}(r))| \qquad r \in \{2, 7, 23, 57\} \tag{20}$$

where the features are selected to discriminate between successive class pairs clean-pipe, cracks, holes joints, laterals, and pipe-collapse. A further set of four features is chosen based on rectangular structuring elements:

$$a_{\mathrm{J}}(l) = |t(I \circ S_{\mathrm{H}}(l))| \qquad l \in \{2, 47, 121, 155\} \tag{19}$$

selected to discriminate between successive pairs of clean-pipe, cracks-holes, laterals, joints, and pipe-collapse.

Table 1
Appropriate threshold selected for classification of various objects in the underground pipe images by circular structuring element

Threshold values for classification by circular structuring element					Classified class
No.	$A_R(2)$	$A_R(7)$	$A_R(23)$	$A_R(57)$	
1	<150				Clean pipe
2	>150	<1000			Crack
3	>150	>1000	<1700		Hole/joint
4	>150	>1000	>1700	<3150	Lateral
5	>150	>1000	>1700	>3150	Collapse pipe

Table 2
Appropriate threshold selected for classification of various objects in the underground pipe images by horizontal structuring element

Threshold values for classification by horizontal structuring element					Classified class
No.	$A_L(2)$	$A_L(47)$	$A_L(121)$	$A_L(155)$	
1	<150				Clean pipe
2	>150	<1000			Crack/hole
3	>150	>1000	<1700		Lateral
4	>150	>1000	>1700	<3150	Collapse pipe
5	>150	>1000	>1700	>3150	Joint

The classifier is then made up of pairwise discriminants, such as

$$a_{\mathrm{L}}(l) \underset{\text{Class 2}}{\overset{\text{Class 1}}{\gtrless}} \tau(l) \tag{20}$$

Where the threshold $\tau(l)$ is based on criterion discriminating between two classes. To maximize $D_{i,j}(r)$–the separation of the class means normalized to the standard deviations–the optimum threshold in discriminating classes i and j is the weighted mean

$$\tau_{i,j}(r) = \frac{\sigma_i(r)\mu_i(r) + \sigma_j(r)\mu_i(r)}{\sigma_i(r) + \sigma_j(r)}, \text{ thus} \tag{21}$$

$$\tau_{0,1}(r) = \frac{\sigma_{\mathrm{crack}}(r)\mu_{\mathrm{clean}}(r) + \sigma_{\mathrm{clean}}(r)\mu_{\mathrm{crack}}(r)}{\sigma_{\mathrm{crack}}(r) + \sigma_{\mathrm{clean}}(r)} \tag{22}$$

The deduced thresholds are listed in Tables 1 and 2. The threshold values shown in Tables 1 and 2 are selected based on the pixel count area of the classified class. For example, segmented collapse pipe image will have the pixel area count of more than 1700 as compared to the segmented crack or hole in the pipe image, which will have pixel area count of less than 1700.

6. Experimental results

We have applied the proposed approach to more than 500 underground concrete sewer pipe images. These images are obtained from SSET inspection of flush-cleaned 18-in. diameter of concrete sewer pipes from various municipalities in North America. Based on the experimental results, we conclude that the proposed method can segment and classify pipe images effectively and accurately. The proposed morphological segmentation and classification algorithm will work very well for under-

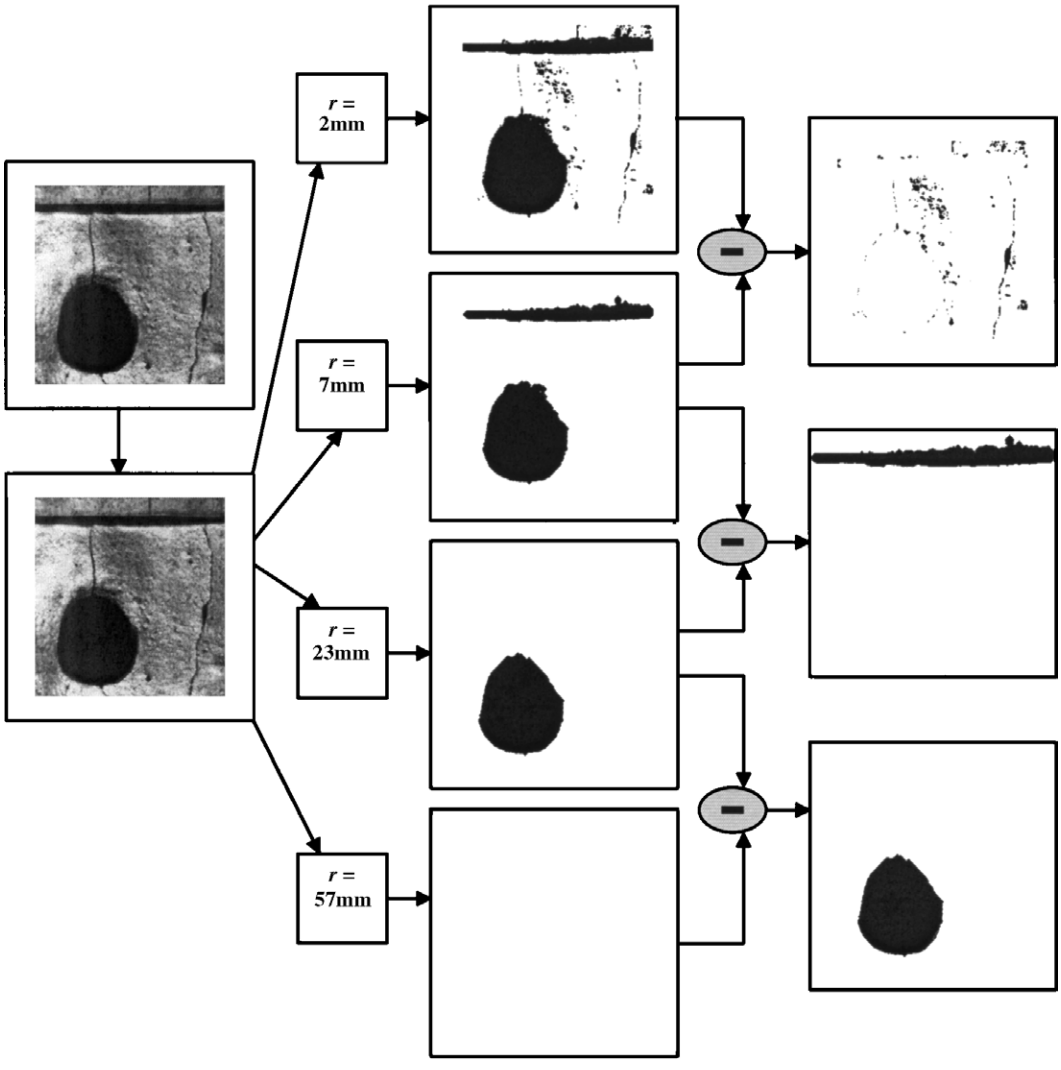

Fig. 11. Classification results by using circular structuring element: the original images are opened by structuring element of different sizes as outlined in Table 1, and finally binary images are obtained by global thresholding technique.

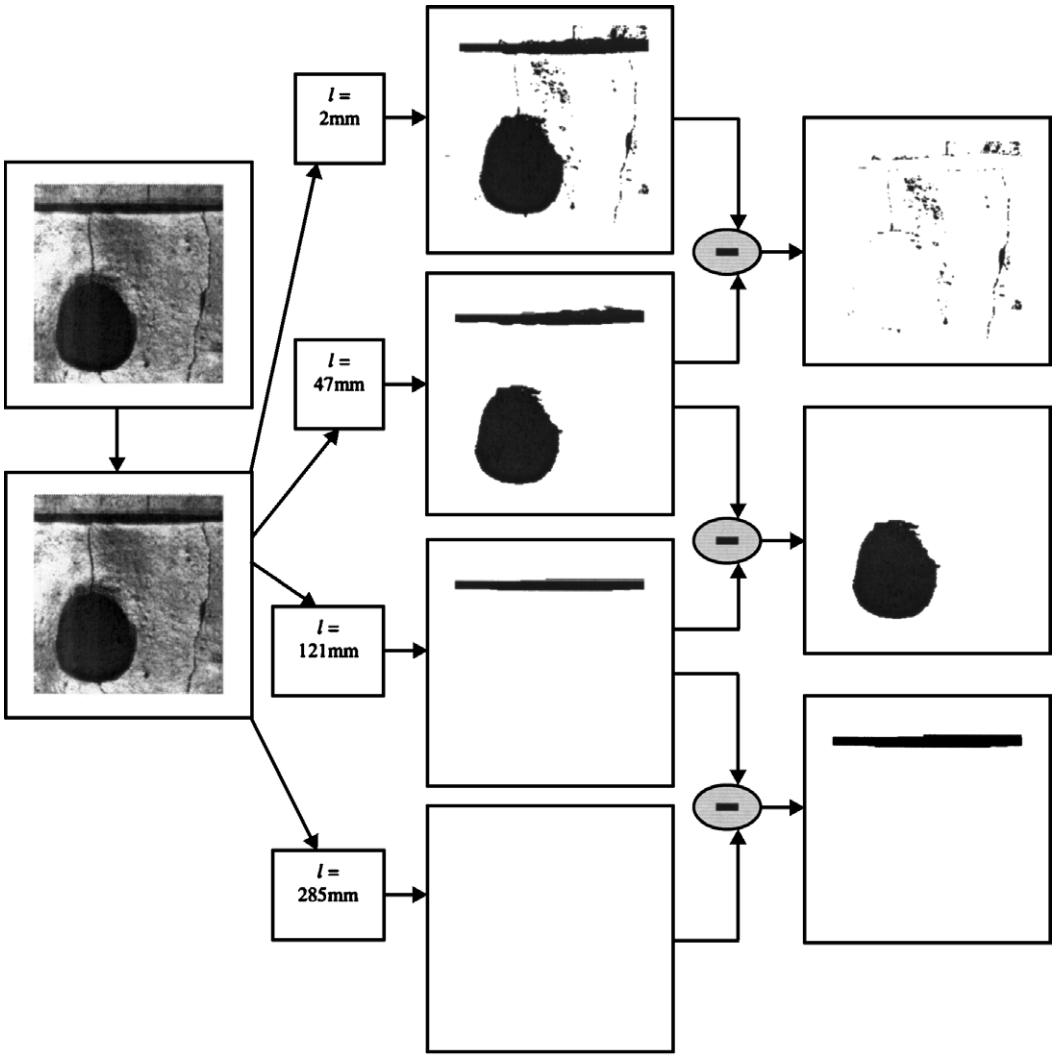

Fig. 12. Classification results by using horizontal structuring element: the original images are opened by structuring element of different sizes as outlined in Table 2, and finally binary images are obtained by global thresholding technique.

ground pipe images containing one class of object only in a given frame. In the real world problem, underground pipe images may contain cluttered objects as shown in Figs. 11(a) and 12(a). For segmentation and classification of such images, we suggest a slightly different approach. The new approach is based on taking the difference of image after each morphological opening and thresholding operations. Figs. 11(c) and 12(c) illustrate the procedure of taking difference of image after successive opening operations to segment various objects present in the image. Once the objects are segmented, then feature extraction and classification can be done.

Table 3
Confusion matrix using the circular structuring element as classifier (row—morphological classifier results and column—expert labeling)

Class	Clean pipe	Crack	Hole/joint	Laterals	Pipe collapse	Total	Percent correct
	1	2	3	4	5		
1	50	0	0	0	0	50	100
2	0	85	15	0	0	100	85
3	0	0	95	5	0	100	95
4	0	0	1	47	2	50	94
5	0	0	0	4	21	25	84
Total	50	85	111	56	23	325	
		Overall percentage correct classification					91.7

Table 4
Confusion matrix using the horizontal structuring element as classifier (row—morphological classifier results and column—expert labeling)

Class	Clean pipe	Crack/hole	Lateral	Pipe collapse	Joints	Total	Percent correct
	1	2	3	4	5		
1	49	0	0	0	1	50	98
2	0	141	0	0	9	150	94
3	0	0	48	0	2	50	96
4	0	0	0	24	1	25	96
5	0	0	0	0	50	50	100
Total	49	141	48	24	63	325	
		Overall percentage correct classification					96

We may evaluate the performance of proposed segmentation and classification methods by a confusion matrix indicating whether the classification tendency is reasonable or not. On the confusion matrix, if we have a normal distributed matrix with few outliers, centered on the diagonal, the classification can be said to be reasonable. Tables 3 and 4 show the agreement and disagreement between the expert classification and the proposed classifier in terms of confusion matrix by using circular and horizontal structuring elements, respectively.

7. Conclusions

We have demonstrated an image processing and morphological approach to segment and classify images of underground concrete pipes. Experimental results demonstrate that the proposed approach is effective for dealing with the underground pipe images with varying background pattern and non-uniform illumination. Morphological segmentation approach can be used to distinguish between cracks, holes, laterals and joints, but it is difficult to classify these objects into various classes based on their severity of defects. Therefore, the segmented joints and laterals have to be further processed to be classified according to the severity of defects by using other shape or textural features, like roundness, compactness, etc. Again, the cracks in pipe images are extracted and classified well by the morphological segmentation approach, but the crack pixels are not detected precisely. Once the laterals, joints and holes are segmented and classified from the image then the crack detection ,filters, as described in [32–34], can be used for precise detection of crack features.

References

[1] T. Iseley, D.M. Abraham, S. Gokhale, Intelligent sewer condition evaluation technologies, Proc. of Intl. NO-DIG Conf., 1997, pp. 254–265.

[2] R. Wirahadikusumah, D.M. Abraham, T. Iseley, R.K. Prasanth, Assessment technologies for sewer system rehabilitation, Journal of Automation in Construction 7 (4) (1998) 259–270.

[3] T. Iseley, Pipeline condition assessment: achieving uniform defect ratings, Proc. of Infra 99 Intl. Conf., vol. 1, 1999, pp. 121–132.

[4] G.J. Agin, Computer vision systems for industrial inspection and assembly, Journal of Computer (1980) 11–20.

[5] A. Rosenfeld, A.C. Kak, Digital Picture Processing, Academic Press, NY, 1982.

[6] K.R. Castleman, Digital Image Processing, Prentice-Hall, Inc., New Jersey, 1996.

[7] M.J. McDonnell, Box filtering techniques, Computer Graphics and Image Processing 17 (3) (1981) 65–70.

[8] A.R. Smith, Color gamut transform, Computer Graphics 12 (3) (1978) 12–19.

[9] W.K. Pratt, Digital Image Processing, Wiley, New York, 1978.

[10] R.O. Duda, P.E. Hart, Pattern Classification and Scene Analysis, Wiley Publication, New York, 1970, pp. 271–272.

[11] A.S. Abutaleb, Automatic thresholding of gray-level pictures using two-dimensional entropy, Computer Vision, Graphics, and Image Processing 47 (1989) 22–32.

[12] J.A. Acosta, J.L. Figueroa, R.L. Mullen, Feasibility study to implement the video image processing technique, Automated Pavement Distress, FHWA, Iowa, 1992.

[13] J.F. Canny, A computational approach to edge detection, IEEE Transactions on Pattern Analysis and Machine Intelligence 8 (6) (1986) 679–698.

[14] S.Y. Chen, W.C. Lin, C.T. Chen, Split and merge image segmentation based on localized feature analysis and statistical tests, CVGIP. Graphical Models and Image Processing 53 (5) (1991) 457–475.

[15] R.C. Gonzalez, P. Wintz, Digital Image Processing, Addison-Wesley Publishing Co, Reading, Massachusetts, 1987.

[16] P.K. Sahoo, S. Soltani, A.K.C. Wong, A survey of thresholding techniques, Computer Vision, Graphics, and Image Processing 41 (2) (1988) 233–260.

[17] K.R. Maser, Computational Techniques for Automating Visual Inspection, Massachusetts Institute of Technology, Report, Cambridge, MA, 1987.

[18] K.B. Chen, S. Soetandio, R.L. Lytton, Distress identification by an automatic thresholding technique, Proc. of Intl. Conf. on Application of Advanced Technologies in Transportation Engineering, San Diego, 1989.

[19] J. Kittler, J. Illingworth, J. Foglein, K. Parker, An automated thresholding algorithm and its performance, Proceedings - International Conference on Pattern Recognition (1984) 287–289.

[20] M.H. Mohajeri, P.J. Manning, ARIA: an operating system of pavement distress diagnosis by image processing, Transp. Res. Record, vol. 1311, Transportation Research Board, Washington, DC, 1991, pp. 120–130.

[21] F.V.D. Heijden, Image Based Measurement Systems, John Wiley & Sons, NY, 1994.

[22] J.C. Cheng, H.S. Don, Segmentation of Bi-Level Images: A Morphological Approach, World Scientific Publishing Co., Singapore, 1991.

[23] R.M. Haralick, S.R. Stenberg, X. Zhuany, Image analysis using mathematical morphology, Pattern Analysis and Machine Intelligence 9 (4) (1987) 532–550.

[24] H.T.A.M. Heijmans, Morphological Image Operators, Academic Press, MA, 1994.

[25] G. Matheron, Random Sets and Integral Geometry, Wiley, New York, 1975.

[26] J. Sera, Introduction to mathematical morphology, Computer Vision, Graphics, and Image Processing 35 (1986) 283–305.

[27] R.M. Haralick, L.G. Shapiro, Computer and Robot Vision, vol. 1, Addison-Wesley, Reading, MA, 1992.

[28] A.D. Brink, Gray-level thresholding of images using a correlation criterion, IEEE Pattern Recognition Letters 9 (5) (1989) 335–341.

[29] W.N. Lie, Automatic target segmentation by locally adaptive image thresholding, IEEE Transactions on Image Processing 4 (1995) 1036–1041.

[30] N. Otsu, A threshold selection method from gray-scale histogram, IEEE Transactions on Systems, Man, and Cybernetics 9 (1) (1979) 62–66.

[31] J.P. Parker, Gray-level thresholding in badly illuminated images, IEEE Transactions on Pattern Analysis and Machine Intelligence 13 (1) (1991) 813–819.

[32] S.K. Sinha, Automated underground pipe inspection using a unified image processing and artificial intelligence methodology, PhD thesis, University of Waterloo (2000).

[33] P.W. Fieguth, S.K. Sinha, Automated analysis and detection of cracks in underground scanned pipes, IEEE Image Processing Conf., Japan, 1999 (CD-ROM 28AP5A.2).

[34] S.K. Sinha, P.W. Fieguth, Automated detection of cracks in buried concrete pipe images. Automation in Construction 15 (2005) 58–72.

[35] P. Soille, Morphological Image Analysis, Principles and Applications, second ed., Springer-Verlag, Germany, 2003.